



The impact of curved satellite tracks on SAR focusing

Mohr, Johan Jacob; Madsen, Søren Nørvang

Published in:

Proceedings of IEEE 2000 International Geoscience and Remote Sensing Symposium

Link to article, DOI:

[10.1109/IGARSS.2000.860430](https://doi.org/10.1109/IGARSS.2000.860430)

Publication date:

2000

Document Version

Publisher's PDF, also known as Version of record

[Link back to DTU Orbit](#)

Citation (APA):

Mohr, J. J., & Madsen, S. N. (2000). The impact of curved satellite tracks on SAR focusing. In *Proceedings of IEEE 2000 International Geoscience and Remote Sensing Symposium* (Vol. 1, pp. 87-92). IEEE.
<https://doi.org/10.1109/IGARSS.2000.860430>

General rights

Copyright and moral rights for the publications made accessible in the public portal are retained by the authors and/or other copyright owners and it is a condition of accessing publications that users recognise and abide by the legal requirements associated with these rights.

- Users may download and print one copy of any publication from the public portal for the purpose of private study or research.
- You may not further distribute the material or use it for any profit-making activity or commercial gain
- You may freely distribute the URL identifying the publication in the public portal

If you believe that this document breaches copyright please contact us providing details, and we will remove access to the work immediately and investigate your claim.

The Impact of Curved Satellite Tracks on SAR Focusing

Johan Jacob Mohr and Søren Nørvang Madsen
 Dept. of Electromagnetic Systems, Technical University of Denmark
 Ørsted's Plads, Build. 348, DK-2800 Kgs. Lyngby, Denmark
 Phone: +45 4525 3800 / Fax: +45 4593 1634 / E-mail: jm@emi.dtu.dk

ABSTRACT

This paper addresses the geometric effect of processing single look complex synthetic aperture radar (SAR) data to a reference squint angle different from that given by the center of the real antenna beam. For data acquired on a straight flight line, the required transformation of radar coordinates from one Doppler reference to another is independent of the target elevation but for data acquired from a satellite orbit over a rotating Earth that is not true. Also the effect of ignoring Earth rotation is addressed.

INTRODUCTION

For large scale exploitation of satellite synthetic aperture radar (SAR) data geometric fidelity is often important. With the European Space Agency ERS-1/2 satellites it has been demonstrated that slant range images can be characterized geometrically with an accuracy corresponding to 10 m on ground by using a dead-reckoning approach, [1]. The final geocoding accuracy for conventional SAR brightness images depends on the accuracy of the digital elevation model used. For SAR products, geocoded using interferometric information, the accuracy depends on the scene and on the acquisition conditions (baseline, atmosphere, etc.) By paying attention to processing fidelity even current satellite SARs support a geometric accuracy on the order of 10 m without use of ground control points.

This paper addresses the impact of geometrically referencing SAR data to a zero Doppler geometry when the platform path is curved and the terrain elevation is unknown. The paper also addresses the large azimuth shift which occur if the horizontal curvature of the orbit due to Earth rotation is ignored.

GEOLOCATION OF SAR IMAGES

The fundamental equations characterizing the geometry of slant range SAR images are the range and Doppler equations

$$R = |\bar{R}_s - \bar{R}_t| \quad (1)$$

$$f_D = -\frac{2}{\lambda R} (\bar{V}_s - \bar{V}_t) \cdot (\bar{R}_s - \bar{R}_t) \quad (2)$$

where R is the range, f_D the Doppler frequency, \bar{R} a position vector, \bar{V} a velocity vector, λ the wavelength, and indices s and t denotes satellite and target, respectively, e.g. [2].

The analysis presented in this paper uses an Earth body fixed coordinate system, i.e. the target velocity is zero. Also, the

Doppler frequency, f_D , is expressed as the squint angle, ψ , between the plane orthogonal to the velocity vector and the line-of-sight vector.

LINEAR SENSOR PATH

For a linear flight track slant-range images can be transformed between different viewing geometries without knowledge of target heights, [3]. An important special case is that a SAR image acquired on a straight flight track, independent of the squint at acquisition, can be transformed to a zero-Doppler geometry. The relevant transformations are

$$r_0 = r_1 \cos \psi_1 = r_2 \cos \psi_2 \quad (3a)$$

$$r_0 = -s_1 \cot \psi_1 = -s_2 \cot \psi_2 \quad (3b)$$

where r denotes slant range, s the along track coordinate, and r_0 is the closest approach distance. The key to the equations is that the axis of the Doppler cone does not change with s .

The implication is that knowledge of the acquisition squint angle is not required for geocoding, only the reference squint angle, utilized in the processing (often zero) is required.

SATELLITE ORBITS

Near circular satellite orbits, $\bar{p}(s)$, have a curvature, κ_v , in the vertical plane of approximately $\kappa_v \approx 1/(R_e + H)$, where R_e denotes the Earth radius and H the satellite height. The orbit also have a curvature, κ_h , in the horizontal plane due to Earth rotation. In polar regions $\kappa_h \approx 0.15\kappa_v$ (for ERS and Radarsat) decreasing to zero near the equator.

We use a circular orbit approximation fitted to the orbit at a reference point, $\bar{p}(s_0)$, such that the unit tangent vectors of the reference and the actual tracks, \hat{t}_0 , coincide, the unit vectors, \hat{b}_0 (out of orbit plane) and \hat{n}_0 (in-plane), coincide (i.e. identical osculation planes), and the curvatures, $\kappa(s_0)$, are identical. The unit vectors ($\hat{t}_0, \hat{n}_0, \hat{b}_0$) are given by, [4],

$$\hat{t}_0 = \frac{\bar{p}'(s_0)}{|\bar{p}'(s_0)|} \quad (4a)$$

$$\hat{b}_0 = \frac{\bar{p}'(s_0) \times \bar{p}''(s_0)}{|\bar{p}'(s_0) \times \bar{p}''(s_0)|} \quad (4b)$$

$$\hat{n}_0 = \hat{b}_0 \times \hat{t}_0 \quad (4c)$$

With $R_\kappa = 1/\kappa(s_0)$, a natural representation of the orbit model,

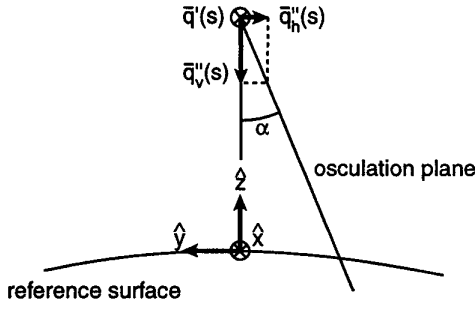


Fig. 1: Satellite orbit $\bar{q}(s)$ with an acceleration (curvature) in both the vertical direction, $\bar{q}''_v(s)$, and the horizontal direction, $\bar{q}''_h(s)$. The osculation plane of the orbit has an angle, α , with the vertical.

$\bar{q}(s)$, can be written as

$$\bar{q}(s) = R_\kappa \sin \frac{s}{R_\kappa} \hat{t}_0 + R_\kappa (1 - \cos \frac{s}{R_\kappa}) \hat{n}_0 \quad (5)$$

see Fig. 1. Note that the plane containing $\bar{q}(s)$ will in general not contain the nadir point. For ERS the osculation plane is rotated at most $9^\circ \approx \arctan 0.15$ relative to the vertical.

CURVED SENSOR PATH

For a curved flight track, slant-range images cannot be transformed to other viewing geometries without knowledge of target heights. In this section equations for transferring data acquired at (r, s) with a squint ψ to zero-Doppler (r_0, s_0) image coordinates are derived, and the sensitivity to look direction variations discussed.

The sensor path is approximated by (5). A coordinate system with $\hat{x} = \hat{t}_0$, $\hat{y} = \hat{b}_0$, and $\hat{z} = -\hat{n}_0$ is used, see Fig. 2. The origin of the s -coordinate is, contrary to (3), chosen so that $s = 0$ corresponds to observing the target at the squint-angle ψ . Assuming a right-looking system the sensor to target vector can be written as

$$\bar{r} = \begin{pmatrix} r_x \\ r_y \\ r_z \end{pmatrix} = r \begin{pmatrix} \sin \psi \\ -\cos \psi \sin \theta \\ -\cos \psi \cos \theta \end{pmatrix} \quad (6)$$

where θ is the look-angle relative to the osculation plane of the orbit.

Closest approach – known target height

The length of the projection of the center-of-curvature to target vector onto the (x, z) -plane is

$$R_{xz} = \sqrt{(R_\kappa + r_z)^2 + r_x^2} \quad (7)$$

By inspecting Fig. 2 the along-track coordinate, s_0 , corresponding to closest approach is found to be

$$s_0 = R_\kappa \arctan \frac{r_x}{R_\kappa + r_z} \quad (8)$$

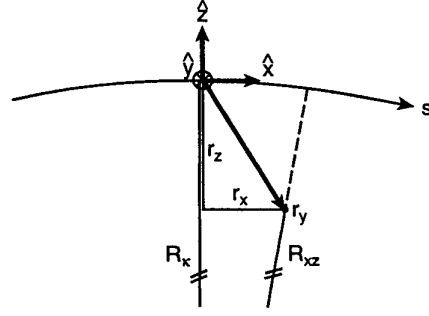


Fig. 2: Satellite track with a radius of curvature, R_κ , approximated by a circle in the osculation plane (x, z) , where $\hat{x} = \hat{t}_0$, $\hat{y} = \hat{b}_0$, and $\hat{z} = -\hat{n}_0$. A target is assumed at a known position (r_x, r_y, r_z) .

where $r_z < 0$. Again, using Fig. 2, the closest approach distance, r_0 , is found to be

$$r_0 = \sqrt{(R_\kappa - R_{xz})^2 + r_y^2} \quad (9)$$

Thus, in transferring (r, s, ψ) to a zero-Doppler geometry r_0 is given by (9), and s is shifted by s_0 given by (8).

Closest approach – unknown target height

The partial derivatives of the sensor target vector \bar{r} with respect to θ is

$$\frac{\partial \bar{r}}{\partial \theta} = \begin{pmatrix} 0 \\ -r \cos \psi \cos \theta \\ r \cos \psi \sin \theta \end{pmatrix} = \begin{pmatrix} 0 \\ r_z \\ -r_y \end{pmatrix} \quad (10)$$

Using (8), (10), and (6) it is seen that

$$\begin{aligned} \frac{\partial s_0}{\partial \theta} &= \frac{\partial s_0}{\partial r_z} \frac{\partial r_z}{\partial \theta} = \frac{R_\kappa r_y}{R_{xz}^2} r_x \\ &= -\frac{R_\kappa r^2 \sin \theta}{2R_{xz}^2} \sin 2\psi \end{aligned} \quad (11)$$

This shows that to first order, the along track error caused by not knowing the target height is a linear function in ψ . Using (9), (7), and (10) the partial derivatives of the closest approach distance with respect to θ are found

$$\begin{aligned} \frac{\partial r_0}{\partial \theta} &= \frac{\partial r_0}{\partial r_y} \frac{\partial r_y}{\partial \theta} + \frac{\partial r_0}{\partial R_{xz}} \left(\frac{\partial R_{xz}}{\partial r_x} \frac{\partial r_x}{\partial \theta} + \frac{\partial R_{xz}}{\partial r_z} \frac{\partial r_z}{\partial \theta} \right) \\ &= -R_\kappa \frac{r_y}{r_0} \left(1 - \frac{R_\kappa + r_z}{R_{xz}} \right) \\ &\approx \sin \theta_0 \frac{s_0^2}{2R_\kappa} \end{aligned} \quad (12)$$

where θ_0 is the look angle at closest approach. It is seen that to first order, the slant range error caused by not knowing the target height is a quadratic function in ψ .

Table 1: Image shifts s_0 (along-track) and $r - r_0$ (slant-range) for a transformation from a squint angle ψ to a zero-Doppler geometry. An ERS geometry with $H = 790$ km, $r = 850$ km, near equator is used, ($\kappa_h = 0$). The transformation errors, Δ_s and Δ_r , are for a target offset 2000 m from the reference sphere, $R_e = 6370$ km.

Impact of a 2000 m target height				
ψ [deg]	s_0 [m]	$r - r_0$ [m]	Δ_s [m]	Δ_r [m]
0.1°	1669	1.5	-0.46	0.0004
3.0°	50055	1311.9	-13.89	0.3633

To describe the impact of not knowing the target elevation, the along-track error, Δ_s , and the slant-range error, Δ_r , are calculated for a 2000 m elevation error when going from the squint angles $\psi = 0.1^\circ$ and $\psi = 3.0^\circ$ to a zero-Doppler geometry, see Table 1. For a C-band SAR at a 790 km altitude the squint angles corresponds to Doppler frequencies of 460 Hz (yaw-steered ERS example) and 13880 Hz (non yaw-steered satellite, e.g. Radarsat or JERS-1). The target offset of 2000 m from the reference sphere corresponds to $\Delta\theta \approx 0.35^\circ$.

It is seen that for ERS, it is not critical to know the target height. For Radarsat, though, the effect is pronounced. Also note, that the difference between an ellipsoidal Earth model and a local spherical approximation is much smaller than typical height variations in the terrain.

EARTH ROTATION – HORIZONTAL CURVATURE

During focusing both the vertical orbit curvature, κ_v , and the horizontal curvature, κ_h , should be accounted for. If not de-focusing will occur, but also transformation between squint angles cannot be done properly.

The orbit curvature, R_κ , and rotation, α , of the osculation plane of the orbit is

$$R_\kappa = \frac{1}{\sqrt{\kappa_v^2 + \kappa_h^2}} = \frac{1}{\kappa_v \sqrt{1 + c_\kappa^2}} \quad (13)$$

$$\alpha = \tan c_\kappa \quad (14)$$

where $c_\kappa = \kappa_h/\kappa_v$, see Fig. 1. The combined effect of using a wrong radius of curvature and a wrong orientation of the osculation plane are shown in Table 2 for a horizontal curvature typical for ERS near the poles, i.e. $c_\kappa = 0.15$.

Radius of curvature

By calculating the first and second order partial derivatives of (8) with respect to c_κ , a weak quadratic dependence on c_κ is found. To first order the dependence on ψ is linear. For $\psi = 0.1^\circ$, $c_\kappa = \pm 0.15$, and the parameters from Table 1 the

Table 2: Image shifts s_0 (along-track) and $r - r_0$ (slant-range) for a transformation from a squint angle ψ to a zero-Doppler geometry for ERS data near the poles, ($c_\kappa = 0.15$). The transformation errors, Δ_s and Δ_r , arise if the horizontal curvature is ignored. Otherwise, the geometry and radar parameters equals those used for Table 1.

Horizontal orbit curvature ($c_\kappa = 0.15$)				
ψ [deg]	s_0 [m]	$r - r_0$ [m]	Δ_s [m]	Δ_r [m]
0.1°	1681	1.5	11.8	-0.010
3.0°	50406	1320.1	350.5	-9.187

along track mis-location is found to be 2.4 m.

Orientation of osculation plane

Ignoring the $\pm 9^\circ$ variations of the orientation of the osculation plane of the orbit due to the horizontal orbit curvature corresponds to up to a factor 30 larger θ variations than unknown terrain. This causes ± 10 m along track mis-locations even for a small squint of 0.1° as for ERS. This is of the same order of magnitude as the combined effect of all other along track error sources, [1].

CONCLUSIONS

Equations for transformation of data acquired with squint to a zero-Doppler geometry are derived. For satellites, the transformation depends on the squint angle and the look angle between the osculation plane of the orbit and the target. An unknown target height is not a concern for the yaw-steered ERS, but should be considered for non yaw-steered systems if the highest geometrical accuracy is required. In both cases, Earth rotation has to be taken into account in the along-track transformation of data to a zero-Doppler geometry, in order to keep the error well below 10 m.

REFERENCES

- [1] J.J. Mohr and S.N. Madsen, "Automatic generation of large scale ERS DEMs and displacement maps," in <http://www.esrin.esa.it/fringe99>, Liege, Belgium, 1999.
- [2] J.C. Curlander, "Location of spaceborne SAR imagery," *IEEE Trans. on Geoscience and Remote Sensing*, vol. 20, no. 3, pp. 359–364, July 1982.
- [3] S.N. Madsen and H. Zebker, "Imaging radar interferometry," in *Manual of Remote Sensing*, Floyd. M. Henderson and Anthony J. Lewis, Eds., vol. 2, chapter 6, pp. 359–380. John Wiley & Sons, Inc., 3rd edition, 1998.
- [4] G.A. Korn and T.M. Korn, *Mathematical Handbook for Scientist and Engineers*, McGraw-Hill Book Company, Inc., 1961.